

# Articles

## Triplet Excitation Energy Transfer as a Function of Concentration in Glassy Methylbenzophenone

Hyoung-Soon Han, Jae-Kwang Lee, Kye-Chun Nam,  
Yong-Kook Choi, and Seong-Keun Kook\*

Department of Chemistry Chonnam National University, Kwangju 500-757, Korea  
Received February 10, 1998

Spectral diffusion following direct triplet excitation from the ground state in glassy Methylbenzophenone as a function of transition energy has been studied. The concentrations of donor and acceptor have been determined for different transition energies. The geometrical distribution was determined by a computer simulation. The cluster size increases gradually with concentration and cluster percolation is observed at 0.31 mole fraction for a three dimensional system. The average distance between a donor and an acceptor also has been determined for different concentrations. The energy transfer efficiency changes abruptly at a critical concentration of 0.054, corresponding to a critical distance of 9.8 Å. The  $\gamma$  value was evaluated to be 1.17.

### Introduction

The mechanisms of electronic energy transfer in condensed molecular system have long been an interesting topic of research, both in experiment and in theory. The theories of energy transfer have been discussed in terms of different interaction mechanisms, e. g., multipolar interaction, exchange coupling, and superexchange tunneling.<sup>1-3</sup> Recent theoretical and experimental investigations have focused in disordered system. Inokuti and Hirayama<sup>4</sup> formulated a theory involving the isotropic exchange interaction for direct (single step) triplet state transfer from a donor to randomly distributed acceptors in three dimensions. This theory later was generalized to all dimensions, and a configuration average valid for all acceptor concentrations was introduced.<sup>5</sup>

Spectral diffusion can be defined as the process of energy transfer between molecules that have different transition energies in a single-component energy transfer system. The distribution of transition energies, which is called inhomogeneous broadening, results from the different local environments or disorder of the molecules in the sample. For the case where the inhomogeneous width is less than  $kT$ , spectral diffusion causes an initially sharp excitation line to broaden to the full inhomogeneous width. For the case where the inhomogeneous width is greater than  $kT$ , spectral diffusion causes relaxation to lower energy molecules or sites. Parson and Kopelman<sup>6</sup> studied theoretically the migration of incoherent excitations in energetically disordered systems using a self-consistent diagrammatic approximation. Spatial diffusion and energy relaxation observables are related to the solution of a nonlinear integral equation. The dependence of spatial and spectral transport properties upon the spatial range and the energy dependence of the intermolecular hopping rate are examined. The intimate relationship between spatial transport and energy relaxation is discussed in detail.

Experimental studies of spectral diffusion generally have

measured luminescence spectra as functions of excitation energy, temperature, concentration, and time. Richert and Bassler<sup>7,8</sup> measured luminescence spectra as a function of time. They reported measurements of the decay of the first vibronic band of the phosphorescence of organic glasses (Benzophenone, Anthraquinone, and Phenanthrene). The triplet state population was created indirectly by intersystem crossing from the singlet manifold. Consequently, the initial distribution of triplet state excitation energies is not known. The data were analyzed in terms of multistep hopping down the cascade of states that form the inhomogeneously broadened band. Jankowiak, Ries and Bassler observed spectral diffusion and triplet exciton localization in glassy 2-bromonaphthalene following direct triplet state excitation.<sup>12</sup> Both the origin of the phosphorescence and the Stokes shift between excitation and phosphorescence varied continuously with excitation energy. The phosphorescence was inhomogeneously broadened and the case of true resonance phosphorescence, characterized by sharp line emission, was not attained. Prasad and coworkers<sup>9-11</sup> observed spectral diffusion in orientationally disordered 4-bromo-4-chlorobenzophenone (BCBP) and in crystalline solutions of 1-bromo-4-chloronaphthalene (BCN) and 1,4-dibromonaphthalene (DBN). The latter system exhibits both orientational and substitutional disorder. For the case of BCBP, time-resolved studies revealed that the phosphorescence profile gradually shifts by a few wavenumbers toward the lower energy sites with increasing time following excitation. This observation implies that the density of acceptor states plays the dominant role in spectral diffusion and not coupling to phonons or vibrons. Park and coworkers<sup>13</sup> determined the cluster distribution by a computer simulation for different concentration of 1,4-dibromonaphthalene (DBN) in 4,4'-dibromobenzophenone (DBBP)/1,4-dibromonaphthalene (DBN) choleic acid to model the energy transfer dynamics. The results showed that the energy transfer efficiency is restricted by single range interaction and the energy transfer rate is reduced by a factor of 15 relative to that in DBBP/

DBN doped into polystyrene due to the larger distance between molecules. Kook and Hanson<sup>14</sup> studied spectral diffusion of triplet excitation in glassy Methylbenzophenone (MBP) as functions of time and concentration. The triplet state was obtained by direct triplet state excitation. At the low excitation energy, the sharp resonant emission line was observed. As the excitation energy increases, the separation between the donor and the acceptor decreases and energy transfer becomes more efficient. Therefore, a broad luminescence band of increasing intensity developed to lower energy and the intensity of the sharp line decreases due to fast spectral diffusion.

These previous studies of spectral diffusion of triplet state in molecular solids have revealed that the geometrical distribution and the separation of molecules play dominant role in energy transfer processes. In the present paper, we report the study of the geometrical distribution and the separation of the molecules as a function of excitation energy for glassy Methylbenzophenone (MBP). The number of donors, acceptors, and barriers depends on the initial excitation energy used. A phosphorescence excitation spectrum for MBP has been obtained to determine the concentrations of donor and acceptor. Energy transfer efficiency ( $\alpha$ ) was obtained for different concentrations of acceptor. Computer simulation was carried out to determine the cluster distribution and to calculate the nearest distance between neighboring molecules for different acceptor concentrations. The data were analyzed in order to determine the values of  $\gamma$ , which characterize the range of the exchange interaction and depend on the overlap of the donor phosphorescence and the acceptor absorption spectra.

### Cluster Distribution and Average distance

A phosphorescence excitation spectrum<sup>14</sup> obtained at 4.2 K for glassy MBP is shown in Figure 1. The phosphorescence was monitored at 4396 Å with band pass of 0.7 Å, and the emission intensity was normalized to account for the vari-

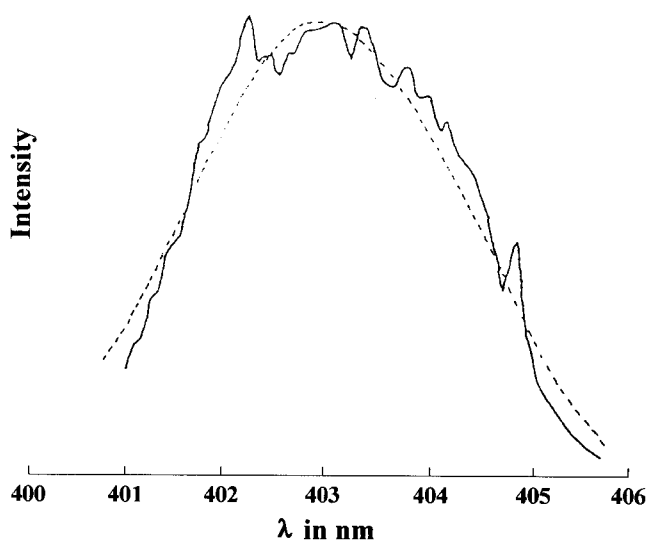


**Figure 1.** Excitation spectrum obtained by monitoring phosphorescence at 4.2 K for glassy MBP. The dotted curve is a Gaussian profile plotted in wavelength centered at 403 nm with a width of 197 cm<sup>-1</sup> (fwhi).

ation in the laser intensity with wavelength. The peak in the excitation spectrum of glassy MBP is at 403 nm with a width of 197 cm<sup>-1</sup> (fwhi). The dotted curve is a Gaussian profile plotted in wavelength centered at 403 nm with a width of 197 cm<sup>-1</sup> (fwhi). The result indicates that the excitation profile is a Gaussian distribution. Upon excitation, the molecules are divided into three classifications: donors—the molecules requiring an excitation energy equal to the initial excitation energy, acceptors—molecules requiring an excitation energy lower than the initial excitation energy, and barriers—molecules requiring an excitation energy higher than the initial excitation energy. We can reasonably assume that the molecules having excitation energies  $\leq v_{ex}$  are the acceptors. As the excitation energy increases, the density of acceptor increases. This increase enhances the energy transfer rate from donors to acceptors. The effective mole fraction of acceptor concentration is then given as<sup>19</sup>

$$Ca(v_{ex}) = \int_{-\infty}^{v_{ex}} I(v)dv / \int_{-\infty}^{\infty} I(v)dv \quad (1)$$

where  $I(v)$  is the absorption profile for the system. Since intensity profile is a Gaussian distribution, we can write

$$Ca(v_{ex}) = (\Delta v)^{-1} (\ln 2/\pi)^{1/2} \int_{-\infty}^{v_{ex}} \exp[-((v - v_{max})/\Delta v)^2] dv \quad (2)$$

Here  $\Delta v$  is the half-width of the distribution (hwhi). The acceptor concentration then can be written in terms of an error function as<sup>10</sup>

$$Ca(v_{ex}) = \frac{1}{2} [1 - \text{erf}(z)], \quad (3)$$

where  $z = (v_{max} - v_{ex})/\Delta v$ ;  $v_{max}$  is the absorption maximum. The acceptor concentrations determined using eq. (3) for different excitation energies are listed in Table 1.

In a similar way, if we assume that the laser profile is Gaussian with hwhi =  $\Delta v_L$ , centered at  $v_{ex}$ , the donor concentration can be written as

$$Cd(v_{ex}) = (\Delta v_L/\Delta v) \exp(-z^2) \quad (4)$$

When the excitation energy is at 4055 Å, using  $\Delta v_L = 0.5$  cm<sup>-1</sup>, the acceptor and the donor concentrations expressed as mole fraction are  $C_a = 0.034$  and  $C_d = 0.00168$ , respectively.

**Table 1.** The acceptor concentration ( $C_a$ ) determined for different excitation energies ( $\lambda_{ex}$ ) and average distance ( $r$ ) between neighbors for each concentrations

| $\lambda_{ex}$ | $c_a$ | $r$ (Å) | $\alpha$ | $\gamma$ |
|----------------|-------|---------|----------|----------|
| 4057           | 0.025 | 12.46   | 0.06     | -        |
| 4053           | 0.050 | 10.04   | 0.18     | -        |
| 4052           | 0.054 | 9.80    | 0.50     | -        |
| 4050           | 0.075 | 8.93    | 0.71     | 1.12     |
| 4049           | 0.085 | 8.61    | 0.79     | 1.15     |
| 4048           | 0.100 | 8.30    | 0.85     | 1.17     |
| 4047           | 0.110 | 8.05    | 0.89     | 1.19     |
| 4046           | 0.125 | 7.86    | 0.93     | 1.19     |
| 4044           | 0.150 | 7.55    | 0.96     | 1.15     |
| 4043           | 0.175 | 7.30    | 0.96     | 1.17     |
| 4041           | 0.200 | 7.12    | 0.96     | 1.18     |

$\alpha$ : energy transfer efficiency.  $\gamma$ : Spectral overlap between donor and acceptor, determined using eqs. (8) and (9).

Now we consider the geometrical distribution of acceptors. The actual geometrical distribution of molecules strongly influences the energy transport. The geometrical distribution was determined by a computer simulation. In the simulation, desired concentrations of acceptors were generated in a three-dimensional lattice and determine the cluster distribution. For  $p=1$ , where  $p$  represents the probability that the lattice is occupied, all sites of the lattice are occupied. For  $p$  smaller than unity, there will be unoccupied lattice sites. The unoccupied spaces will produce a distribution of clusters. The distribution of clusters of various size will be observed at different concentration of the occupying species. For low concentrations, there will be many isolated members, as well as many clusters of two, three, or four members. As the concentration increases, the distribution will contain more and more large clusters until several large clusters coalesce into a maxicluster, *i.e.* a percolation cluster. The cluster multiple labeling technique (CMLT)<sup>15</sup> was used to determine the size of cluster ( $m$ ) and the frequency of the cluster size  $m$  ( $i_m$ ). CMLT technique is based on the application of alternate labels to sites belonging to the same cluster. This technique is appropriate for the determination of the cluster distribution of a finite randomly mixed crystals. The practical algorithm is described in ref. 15. By inspecting the distribution of the cluster size, it can be seen that the cluster size increases gradually and cluster percolation is not observed in the concentrations lower than 25%. Figure 2 shows the average cluster size ( $I_{Av}$ ) for a three-dimensional lattice as a function of concentration. The definition of  $I_{Av}$  is<sup>15,17</sup>

$$I_{Av} = \frac{\sum_m i_m m^2}{\sum_m i_m m} \quad (5)$$

This  $I_{Av}$  increases monotonically with the concentration and diverges at the percolation concentration.<sup>16,17</sup> In a three dimensional system the percolation threshold is found to be 0.31. The critical concentration is a function of topology and decreases with dimensionality. The percolation thresholds in a one and two-dimensional systems are 1.0 and 0.59, respectively.<sup>19</sup>

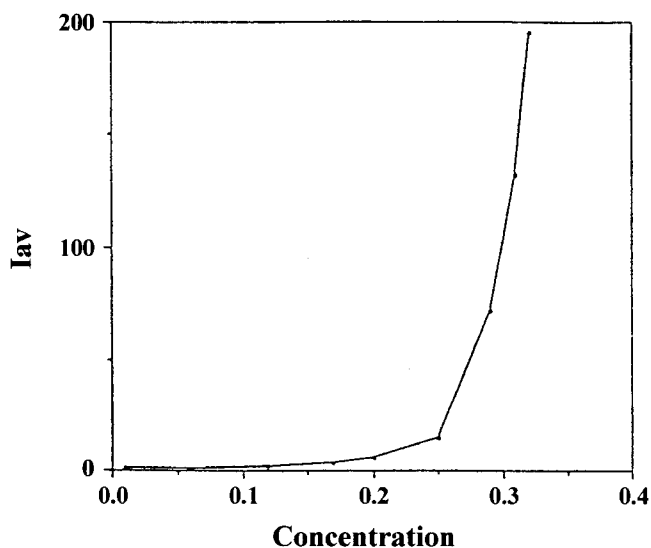


**Figure 2.** Average cluster size  $I_{av}$  as a function of concentration for a three dimensional lattice with  $10^6$  sites. The percolation threshold is 0.31 in three dimension.

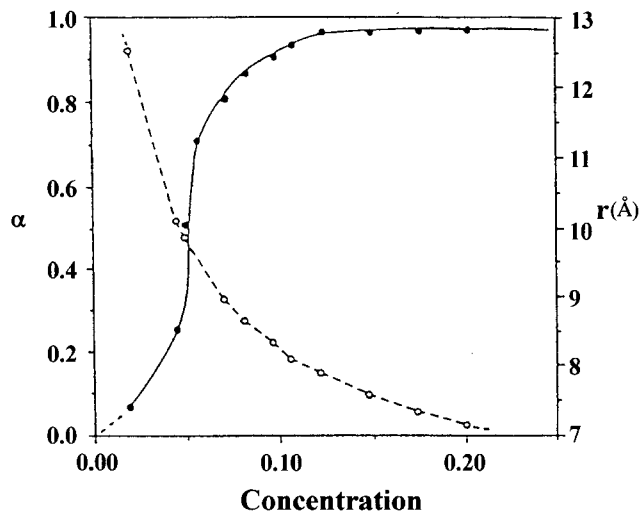


**Figure 3.** A plot of the spectral diffusion efficiency  $\alpha$  versus acceptor concentration of glassy MBP at 4.2 K (solid line). The average distances between neighbors for each concentration also are plotted (dotted line).

A computer simulation was used to determine the average distance between neighboring a donor and an acceptor at different concentrations. In the simulation, molecules were generated in the model space and assigned random coordinates  $x_i, y_i, z_i$ . The nearest-neighbor distance for each molecule was determined by calculating  $[(x_i-x_j)^2+(y_i-y_j)^2+(z_i-z_j)^2]^{1/2}$ . To satisfy the condition that the molecules do not overlap each other, any separation smaller than 4 Å molecular diameter was not allowed. Periodic boundary conditions were used. The average distances between neighbors determined for each concentrations are shown in Table 1 and Figure 3.

### Energy Transfer Efficiency

We now consider the time evolution of excitation at donor sites and acceptor sites. The excitation is generated at the donor sites, and the acceptor population results only by the energy transfer processes from the donor sites. When the excitation visits a acceptor site, it may be captured irreversibly. At  $t=0$ , the number of donor sites  $N_d(0)=N_0$ , and the excitation density of the acceptor sites  $N_a(0)=0$ . The decay of the excited state population of donor and acceptor molecules can be described by simple kinetics,

$$\frac{d N_d}{dt} = -k N_d - k_{ET}(r) N_d + N_0 \quad (6)$$

$$\frac{d N_a}{dt} = -k N_a + k_{ET}(r) N_d \quad (7)$$

where  $N_d$  is the number of donor molecules excited,  $k$  and  $k_{ET}(r)$  are unimolecular decay rate and the energy transfer rate from the donors to the acceptors at a distance  $r$ , respectively. For MBP,  $1/k$  is 2.7 ms.<sup>14,20</sup>  $N_a$  represents the population of acceptors due to excitation transfer from donors.

For the case of transfer, the excitation transport is governed by the exchange interaction. The distance dependence of the energy transfer rate between a donor and an acceptor at distance  $r$  is given as<sup>2</sup>

$$k_{ET}(r) = k \exp[\gamma(d-r)] \quad (8)$$

where  $d$  is the critical transfer distance and  $\gamma$  characterizes the range of the exchange interaction and depends on the overlap of the donor phosphorescence and the acceptor spectra. Under the condition of low donor concentration, donor-donor interactions are neglected. Also any possibility of back transfer from acceptor to donor can be excluded at low temperature. Since the donor and acceptor are the same molecular species, we assume the same quantum yield. Under steady-state conditions, the ratio of the integrated intensity of acceptor emission to the total integrated emission is

$$\alpha = \frac{N_a}{N_a + N_d} = \frac{1}{1 + (k/k_{ET})} \quad (9)$$

Figure 3 shows a plot of the ratio  $\alpha$  versus the acceptor concentration  $C_a$ . As mentioned earlier, the percolation is not observed at the concentrations lower than 0.25. At the concentrations higher than percolation concentration ( $>0.31$ ), the excitation is confined within a cluster size  $m$  and the distance between the neighbors for each molecule is mostly same. Therefore no dependence of the  $\alpha$  on the concentration would be shown. At the concentrations lower than percolation concentration, however, the graph shows the dependence of the spectral diffusion efficiency ( $\alpha$ ) on the density of the acceptor sites. The ratio  $\alpha$  changes abruptly at a critical concentration. The critical concentration (where  $\alpha=0.5$ ) found to be 0.054, and the calculated critical distance is 9.8 Å (see Table 1). At this concentration, the energy transfer rate between a donor to an acceptor equals to the unimolecular decay rate. The abrupt change in  $\alpha$  around the critical concentration is characteristics of a short range exchange interaction. Consequently the exchange interaction mechanism is used to analyze the spectral diffusion.

Now we estimate  $\gamma$  values, which characterize the range of the exchange interaction, for glassy MBP system. First we use eq. (9) to infer  $k_{ET}$  from known  $\alpha$  values in Table 1 for different concentrations. Then with eq. (8), the  $k_{ET}$  values and the average distance ( $r$ ) between neighboring a donor and an acceptor listed in Table 1 are used to determine  $\gamma$  values for different concentrations. Using determined critical distance ( $d=9.8$  Å) and the monomolecular decay rate ( $k=370.37 \text{ sec}^{-1}$ ) for MBP,<sup>14,20</sup> the  $\gamma$  value is evaluated to be 1.17.

### Summary and Conclusions

Spectral diffusion following direct triplet excitation from the ground state in glassy Methylbenzophenone (MBP) as a function of excitation energy is studied. The concentrations of donor and acceptor has been determined using a phosphorescence excitation spectrum for different excitation energies and listed in Table 1. The nearest distance between a donor and an acceptor also has been determined for different concentrations and listed in Table 1. The geometrical distribution was determined by a computer simulation. The cluster size increases gradually and cluster percolation is observed at 0.31 mole fraction for a three dimensional system. The energy transfer efficiency ( $\alpha$ ) is obtained for different

concentrations of acceptor. This experiment reveals that the spectral diffusion efficiency is dependent on the number of acceptors and changes abruptly at a critical concentration of 0.054, corresponding to a critical distance of 9.8 Å. The abrupt change in  $\alpha$  around the critical concentration is characteristics of a short range exchange interaction. The exchange interaction mechanism is used to analyze the spectral diffusion. The value of  $\gamma$ , which characterize the range of the exchange interaction and depends on the overlap of the donor phosphorescence and the acceptor spectra, is determined for exchange interaction and evaluated to be 1.17.

**Acknowledgement** Acknowledgement is made to Basic Science Research Institute Program, administrated by Ministry of Education of Korea (BSRI 97-3429), for support of this research. Partial financial support by CNU Research Foundation is gratefully acknowledged by S.K.

### References

1. Foster, T. *Ann. Physik* **1948**, 2, 55.
2. Dexter, D. L. *J. Chem. Phys.* **1953**, 21, 836.
3. Robinson; G. W.; Nieman, G. C.; *J. Chem. Phys.* **1962**, 37, 2150.
4. Inokuti, M.; Hirayama, F.; *J. Chem. Phys.* **1965**, 43, 1978.
5. Blumen, A.; *J. Chem. Phys.* **1980**, 72, 2632.
6. Parson, R. P.; Kopelman, R. *J. Chem. Phys.* **1985**, 82, 3692.
7. Richert, R.; Bassler, H. *Chem. Phys. Lett.* **1985**, 118, 235.
8. Richert, R.; Bassler, H. *J. Chem. Phys.* **1986**, 84, 3567.
9. Talapatra, G. B.; Rao, D. N.; Prasad, P. N. *J. Phys. Chem.* **1984**, 88, 4636.
10. Talapatra, G. B.; Rao, D. N.; Prasad, P. N. *J. Phys. Chem.* **1985**, 89, 3217.
11. Talapatra, G. B.; Rao, D. N.; Prasad, D. N. *Chem. Phys.* **1986**, 101, 147.
12. Jankowiak, R.; Ries, B.; Bassler, H. *Phys. Stat. sol.* **1984**, 1246, 363.
13. Park, C. H.; Song, C. Y.; Woo, H. G.; Choi, Y. K.; Kook, S. K. *Bull. Korean Chem. Soc.* **1995**, 16, 630.
14. Kook, S. K.; Hanson, D. M.; *Chem. Phys.* **1990**, 146, 303.
15. Hoshen, J.; Kopelman, R. *J. Chem. Phys.* **1976**, 65, 2817.
16. Stauffer, D. *Introduction to Percolation Theory*; Taylor and Francis: London and Philadelphia, 1985; p 52.
17. Francis, A. H.; Kopelman, R. in *Topics in Applied Physics*; Yen, W. M. and Selzer, P. M., Eds.; Springer-Verlag: Berlin Heidelberg, New York, 1981; Vol 49, p 241.
18. Kook, S. K.; Hanson, D. M.; Kopelman, R. *J. Phys. Chem.* **1993**, 97, 12339.
19. Hoshen, J.; Kopelman, R.; Monberg, E. M. *J. Stat. Phys.* **1978**, 19, 219.
20. Lin, Y. Ph. D. Dissertation. Department of Physics, State University of New York at Stony Brook, **1987**.